Kidney International, Vol. 64 (2003), pp. 2–10

GENETIC DISORDERS–DEVELOPMENT

Pathogenesis of nephrogenic diabetes insipidus by aquaporin-2 C-terminus mutations

Tomoki Asai, Michio Kuwahara, Hidetake Kurihara, Tatsuo Sakai, Yoshio Terada, Fumiaki Marumo, and Sei Sasaki

Department of Homeostasis Medicine and Nephrology, Tokyo Medical and Dental University Graduate School, Tokyo, Japan; and Department of Anatomy, Juntendo University School of Medicine, Tokyo, Japan

Pathogenesis of nephrogenic diabetes insipidus by aquaporin-2 C-terminus mutations.

Background. We previously reported three aquaporin-2 (AQP2) gene mutations known to cause autosomal-dominant nephrogenic diabetes insipidus (NDI) (*Am J Hum Genet* 69: 738, 2001). The mutations were found in the C-terminus of AQP2 (721delG, 763 to 772del, and 812 to 818del). The wild-type AQP2 is a 271 amino acid protein, whereas these mutant genes were predicted to encode 330 to 333 amino acid proteins due to the frameshift mutations leading to the creation of a new stop codon 180 nucleotides downstream. The *Xenopus* oocyte expression study suggested that the trafficking of the mutant AQP2s was impaired.

Methods. To determine the cellular pathogenesis of these NDI-causing mutations in mammalian epithelial cells, Madin-Darby canine kidney (MDCK) cells were stably transfected with the wild-type AQP2, or the 763 to 772del mutant AQP2, or both. Cells were grown on the membrane support to examine the localization of AQP2 proteins by immunofluorescence microscopy.

Results. Confocal immunofluorescence microscopy showed that the wild-type AQP2 was expressed in the apical region, whereas the mutant AQP2 was apparently located at the basolateral region. Furthermore, the wild-type and mutant AQP2s were colocalized at the basolateral region when they were cotransfected, suggesting the formation of mixed oligomers and thereby mistargeting.

Conclusion. Mixed oligomers of the wild-type and the 763 to 772del mutant AQP2s are mistargeted to the basolateral membrane due to the dominant-negative effect of the mutant. This defect is very likely to explain the pathogenesis of autosomal-dominant NDI. The mistargeting of the apical membrane protein to the basolateral membrane is a novel molecular pathogenesis of congenital NDI.

By current consensus, aquaporin-2 (AQP2) is known as a vasopressin-regulated water channel confined to the collecting duct cells [1]. There is accumulating evidence that the binding of vasopressin to the V2 receptor at the basolateral membrane initiates intracellular signaling cascades, leading to redistribution of AQP2 from the subapical intracellular vesicle to the apical membrane [2, 3]. Congenital nephrogenic diabetes insipidus (NDI) is a hereditary disease characterized by a lack of responsiveness to vasopressin in the renal collecting tubule. The majority of NDI patients develop the disease due to mutations in the *AVPR2* gene and manifested a pattern of X-linked recessive inheritance [2, 3]. In the autosomal-recessive form of NDI, mutations were detected in the *AQP2* gene [4].

In a recent study, a point mutation (E258K) causing the autosomal-dominant form of NDI was identified in one allele in exon 4 of the *AQP2* gene [5]. This E258K-AQP2 mutant heterotetramerize with the wild-type AQP2, but these tetramers retained in the Golgi compartment in the *Xenopus* oocyte, suggesting that the dominant-negative effect of the mutant causes the autosomal-dominant NDI [5, 6]. We also reported three mutations of the *AQP2* gene responsible for the autosomal-dominant form of NDI [7]. These mutations were also found in a single allele of the *AQP2* gene at the C-terminus: a deletion of G at 721 (721delG), a deletion of 10 nucleotides starting at 763 (763 to 772del), and a deletion of seven nucleotides starting at 812 (812 to 818del). Each of these mutations shifts the stop codon 180 nucleotides downstream. In contrast to the wild-type AQP2 encoding a 271 amino acid protein, these mutants encode 330 to 333 amino acid proteins. Interestingly, all three of these mutants share a common sequence of 61 amino acids at the C-terminal (GRQRPLRPRRTLVR PEAEGPTPSLLSRRSEVGPPAQSSCFLDVRAQAS AVSRRGGG CRREP). Our *Xenopus* oocyte expression study suggested two things: (*1*) that the wild-type and mutant AQP2 proteins form mixed tetramers; and (*2*) that the trafficking to the plasma membrane is impaired in the mixed tetramers due to the dominant-negative

Key words: vasopressin, autosomal-dominant, aquaporin-2.

Received for publication February 7, 2002
and in revised form September 28, 2002, and January 17, 2003
Accepted for publication February 14, 2003

effect of the mutant AQP2. More recently, another AQP2 mutation causing the autosomal-dominant NDI (727delG) was reported [8]. When the wild-type and 727delG AQP2s were cotransfected in Madin-Darby canine kidney (MDCK) cells, the hetero-oligomers of the two AQP2s were predominantly localized at late endosomes/lysosomes [8].

Because our previous study in the autosomal-dominant NDI was performed using *Xenopus* oocytes, a nonpolarized cell type, our findings may not necessarily hold true for mammalian polarized epithelial cells such as renal tubular cells. In this study, we established cell lines that stably express the wild-type AQP2 and one of the mutant AQP2s (763 to 772) to clarify the pathogenesis of our NDI cases. We chose MDCK cells for transfection and the study was focused on the intracellular localization of AQP2 proteins.

METHODS

Preparation of cDNA

The wild-type cDNA of human AQP2 (GenBank accession number NM000486) with a Kozak consensus translation initiation site just upstream of the initial codon (ATG) was inserted into the pcDNA3.1 vector (Invitrogen, CH Groningen, The Netherlands) between the *Hin*dIII site and *Xba*I site. The splicing overlap extension polymerase chain reaction (PCR) technique [9] was used to delete 10 nucleotides starting at 763 from the cDNA of the wild-type human AQP2. In the first PCR step, the template AQP2 DNA was amplified using a 5′ initiation site primer (5′-CCCAAGCTTGCCGCCACCATGTGGGAGCTCCGCTCCATA-3′; underlining and double underlining denote the *Hin*dIII site and Kozak consensus translation initiation site, respectively), an antisense mutation primer (5′-AGGCTCTGCGGCGAGTGCAGCTCCGCCGTCGCA-3′; underlining denotes nucleotides at 752 to 762), a sense mutation primer (5′-GAGCGCGAGGTGCGACGGCGGAGCTGCACTCGC-3′; underlining denotes nucleotides at 773 to 784), and a 3′ end site primer (5′-CCCTCTAGATCAGGGCTCCCTCCGGCAGCC-3′; underlining denotes the *Xba*I site). In the second PCR step, DNA fragment of the 763 to 772del AQP2 was produced by PCR using the 5′ initiation site primer, the 3′ end site primer, and the two first PCR products as templates. The PCR products were digested with *Hin*dIII and *Xba*I, and inserted into the pcDNA3.1/Zeo vector (Invitrogen).

Cell culture and stable transfection

MDCK cells (Japanese Collection of Research Biologicals #9029) were cultured in Dulbecco's modified Eagle's medium (DMEM) (Gibco BRL, Grand Island, NY, USA) supplemented with 10% fetal bovine serum (FBS), 100 U/mL of penicillin, and 100 μg/mL of streptomycin. Cells were grown at 37°C under a humidified 5% CO_2 atmosphere. Ten micrograms of the expression constructs of the wild-type AQP2 and the 763 to 772del mutant were transfected into MDCK cells grown subconfluently on dishes (90 mm in diameter) using the calcium-phosphate precipitation technique. After 24 hours, the cells transfected with the wild-type AQP2 and the mutant AQP2 were trypsinized, split among six dishes, and cultured in DMEM containing 700 μg/mL of G418 (Sigma Chemical Co., St. Louis, MO, USA) and 400 μg/mL of Zeocin (Invitrogen), respectively. Ten to fourteen days after the transfection, individual colonies were selected using cloning rings and expanded. Native vectors were also transfected into MDCK cells as controls. To establish the cotransfected cells, the mutant AQP2 was transfected into the cells stably expressing wild-type AQP2 and cultured in DMEM containing G418 and Zeocin. After the selection, the clones were isolated.

Immunoblot analysis

Transfected cells were homogenized for 30 minutes in RIPA buffer [50 mmol/L Tris-HCl, 150 mmol/L NaCl, 1.0% NP40, 0.5% deoxycholate, 0.1% sodium dodecyl sulfate (SDS), pH 8.0] containing a protease inhibitor cocktail (Boehringer Manheim, Manheim, Germany). The cell lysate was centrifuged at 10,000*g* at 4°C for 30 minutes. The supernatant was denatured in SDS sample buffer at 70°C for 10 minutes. Ten micrograms of total membrane protein were loaded in each lane. The samples were separated by SDS polyacryamide gel electrophoresis (PAGE) and transferred to Immobilon-P filters (Millipore, Bedford, MA, USA) using a semidry system. After blocking the filters overnight in 2% skim milk in TBST solution (20 mmol/L Tris, 150 mmol/L NaCl, 0.05% Triton-X, pH 7.4), they were incubated for 1 hour with either an affinity-purified rabbit antibody against 15 carboxy terminal amino acids of the wild-type or an affinity-purified rat antibody against 15 carboxy terminal amino acids of the mutant AQP2. The filters were then incubated for an additional 1 hour with ^{125}I-protein A solution and examined by autoradiography.

For immunoprecipitation, the membrane fraction of MDCK cells was obtained as described above. Fifty micrograms of the membrane protein were incubated with an antibody against the wild-type or mutant AQP2 for 2 hours at 4°C. Then, protein G agarose (Protein G PLUS-Agarose, Oncogene Science, Uniondale, NY, USA) was added to each sample and incubated for 12 hours at 4°C. After three washes, the samples were denatured, separated by SDS-PAGE, and treated by methods similarly to those described above.

Immunofluorescence microscopy

To detect the localization of proteins in polarized cells, transfected MDCK cells were grown on a permeable supported membrane (Transwell-Clear, Corning, Cambridge, MA, USA). After the 3-day culture in DMEM,

confluent cells were incubated for 2 hours with DMEM containing 10^{-5} mol/L forskolin (Sigma Chemical Co.) to induce the expression of AQP2 to the plasma membrane. In some protocols, cells were not treated with forskolin for comparison. The cells were then fixed for 20 minutes with 2% paraformaldehyde in serum-free DMEM at room temperature, washed with phosphate-buffered saline (PBS), permeabilized with 0.2% Triton X-100 in PBS, blocked with 1% bovine serum albumin (BSA) in PBS at 4°C overnight, and doubly stained. Antibodies against the following proteins were used: the wild-type AQP2 (rabbit or rat, diluted 1:1200), the mutant AQP2 (rabbit, 1:600), a tight junction protein, ZO-1 (mouse, 1:400) (Zymed Laboratories, South San Francisco, CA, USA), a basolateral membrane marker protein, Na-K-ATPase (mouse, 1:400) (Upstate Biotechnology, Lake Placid, NY, USA), and a late endosomal/lysosomal marker protein known as lysosome-associated membrane protein 1 (Lamp1; rabbit, 1:200, kindly provided by Dr. E. Kominami). Cells transfected with the wild-type or the mutant AQP2 were incubated at room temperature for 1 hour with the mixture of two antibodies in PBS containing 1% BSA. After four washes with PBS, the cells were further incubated with a fluorescence-labeled antibody against rabbit immunoglobulin G (IgG) (1:200) (Alexa Fluor 488, Molecular Probes, Eugene, OR, USA), or rat or mouse IgG (1:200) (Alexa Fluor 568, Molecular Probes) for 1 hour. Mock-transfected cells were treated similarly to provide control. After staining, the cells were washed four times with PBS and mounted in a mounting medium (Prolong Antifade Kit, Molecular Probes). Immunofluorescent images of horizontal or vertical sections were obtained with an LSM510 laser scanning confocal microscope system (Carl Zeiss, Jena, Germany) using a 60× water-immersion objective.

To examine the cross reactivity of antibodies against the mutant AQP2 (rabbit) and Na-K-ATPase (mouse), cells transfected with the mutant AQP2 were incubated with antimutant-AQP2 antibody, and then incubated with antibodies against rabbit or mouse IgG. In addition, the same cells were incubated with anti-Na-K-ATPase antibody, and then incubated with anti-mouse or rabbit IgG. The cross reactivity of antibodies against the wild-type AQP2 (rabbit) and Na-K-ATPase (mouse), and the wild-type AQP2 (rat) and mutant AQP2 (rabbit) were tested similarly.

RESULTS

The apparent molecular sizes of the wild-type AQP2 and mutant AQP2 corresponded to 29 kD and 34 kD, respectively [7]. Immunoblots of MDCK cells transfected with the wild-type AQP2 (Fig. 1A) and the mutant AQP2 (Fig. 1B) revealed clear bands at 29 kD and 34 kD, respectively, and broad glycosylated bands at 40 to 50 kD. In contrast, no bands were seen in mock-transfected cells (Fig. 1 A and B). In the immunoblots of cotransfected cells (Fig. 1C), the mixture of two antibodies revealed both 29 kD and 34 kD bands at similar expression levels. These results suggested that the wild-type and/or mutant AQP2s were successfully transfected in MDCK cells.

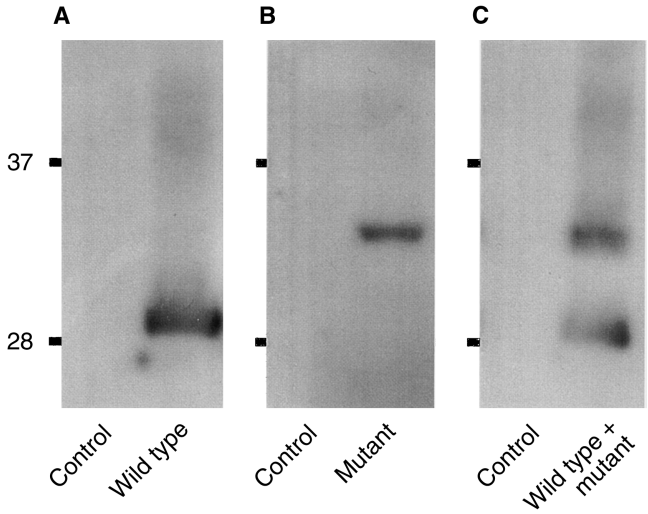

Fig. 1. Immunoblot of membrane fractions of the Madin-Darby canine kidney (MDCK) cells transfected with the wild-type aquaporin-2 (AQP2) (*A*), mutant AQP2 (*B*), and both wild-type and mutant AQP2s (*C*). The protein expression was detected with an affinity-purified antibody against the wild-type (A), mutant AQP2 (B), or a mixture of both (C).

The localization of proteins was examined in polarized MDCK cells by immunofluorescence microscopy. After incubation with forskolin, cells transfected with the wild-type AQP2 were doubly stained with antibodies against the wild-type AQP2 and ZO-1, a tight junction marker. The staining with anti-wild-type AQP2 antibody was almost homogenous in the XY section of each cell, and predominantly localized at the apical side in the XZ section (Fig. 2A). The staining with anti-ZO-1 antibody was found at the apical side of the cell outline, the localization compatible with that of the tight junction (Fig. 2B). The merged figure confirmed the apical distribution of the wild-type AQP2 (Fig. 2C). Figure 2 D and E shows the double staining of the wild-type AQP2 (green) and Na-K-ATPase (red), a basolateral membrane marker, in cells before and after forskolin treatment, respectively. The wild-type AQP2 was mainly distributed at the apical region even without incubation with forskolin (Fig. 2D). Forskolin apparently induced further redistribution of the wild-type AQP2 to the apical membrane (Fig. 2E), suggesting the stimulation of the apical trafficking of AQP2 by forskolin. In contrast to the AQP2-transfected

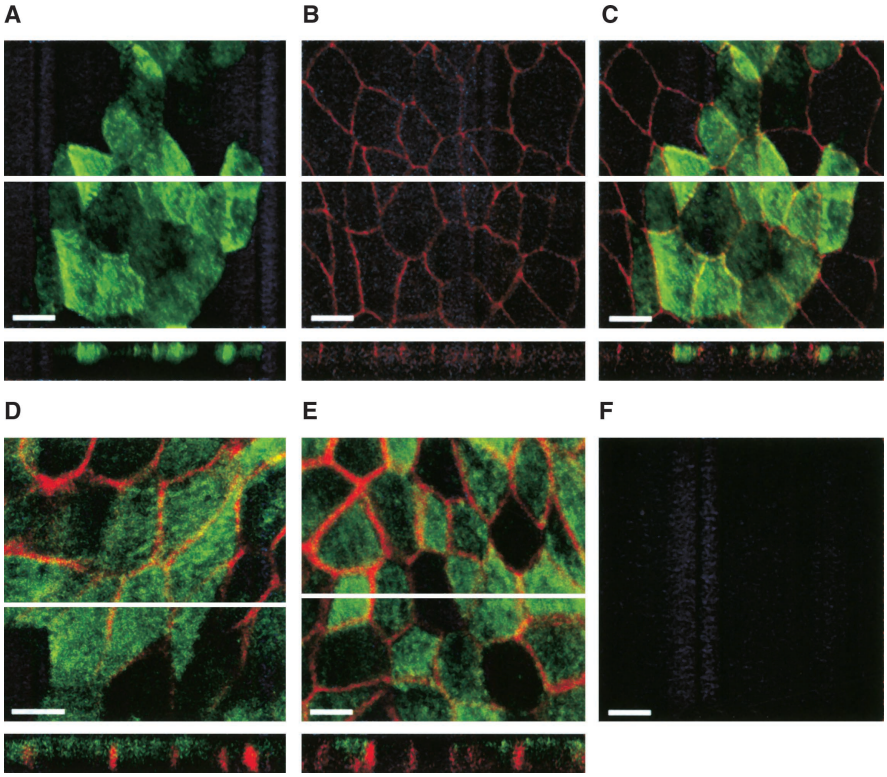

Fig. 2. Immunocytochemical localization of the wild-type aquaporin-2 (AQP2) in Madin-Darby canine kidney (MDCK) cells transfected with the wild-type AQP2 and mock-transfected MDCK cells. The samples were viewed with a confocal microscope at ×400. Localization of the wild-type AQP2 (*A*), ZO-1 (*B*), and merged (*C*). Localization of the wild-type AQP2 and Na-K-ATPase before (*D*) and after forskolin treatment (*E*). Mock-transfected cells (*F*) stained with antibody against the wild-type AQP2. XY and XZ sections are shown in the upper and lower panels, respectively. White bars indicate 10 μm.

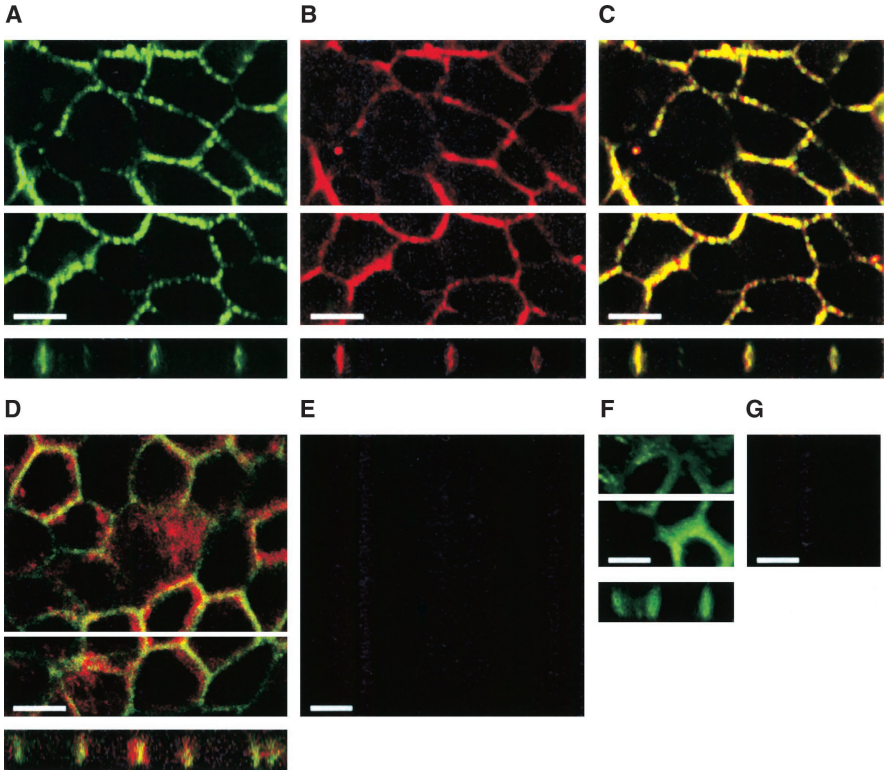

Fig. 3. Immunocytochemical localization of the mutant aquaporin-2 (AQP2) in Madin-Darby canine kidney (MDCK) cells transfected with the mutant AQP2 and mock-transfected MDCK cells. The samples were viewed at ×400X. Localization of the mutant AQP2 (*A*), Na-K-ATPase (*B*), merged with (*C*) or without forskolin treatment (*D*). In contrast to (A to C), the red and green fluorescence represent the staining of the mutant AQP2 and Na-K-ATPase, respectively, in (D). Mock-transfected cells stained with antibody against the mutant AQP2 (*E*). Determination of the cross-reactivity of antibodies. Cells were incubated with rabbit antimutant AQP2 antibody, and then incubated with antibodies against rabbit IgG (*F*) or mouse IgG (*G*). XY and XZ sections are shown in the upper and lower panels, respectively. White bars indicate 10 μm.

cells, no fluorescence from the AQP2 was visible in the mock-transfected cells (Fig. 2F).

In a preliminary study, we noted the conspicuous presence of the mutant AQP2 at the basolateral side. To investigate further, we doubly stained the cells transfected with the mutant AQP2 with antibodies against the mutant AQP2 and Na-K-ATPase after forskolin treatment. The lateral cell surface was brightly stained in the mutant AQP2-expressing cells, whereas the apical signal was negative (Fig. 3A). A weak staining of the basal cell membrane was also visible when the fluorescent image was turned up to high brightness on the monitor (figure not shown). A similar staining pattern was observed in Na-K-ATPase (Fig. 3B). The superimposition of these figures showed the colocalization of these two proteins (Fig. 3C), suggesting that the 763 to 772del mutation is responsible for the mistargeting of the AQP2 protein to the basolateral membrane area. Basolateral localization of the mutant AQP2 was also observed in cells not stimulated with forskolin (Fig. 3D). However, the colocalization of the mutant AQP2 and Na-K-ATPase were seemingly not so close as observed in forskolin-treated cells (Fig. 3C). In contrast to cells expressing the mutant AQP2, no fluorescence was detected in mock-transfected cells (Fig. 3E). Because Figure 3C showed a high overlap of two proteins, the cross-reactivity of two antibodies against the mutant AQP2 (rabbit) and Na-K-ATPase (mouse) was examined. Cells transfected with the mutant AQP2 were incubated with rabbit antimutant AQP2 antibody, and then incubated with anti-rabbit or mouse IgG. The mutant AQP2 was identified by the incubation with anti-rabbit IgG (Fig. 3F), but not with anti-mouse IgG (Fig. 3G), suggesting the cross-reactivity of these antibodies were not responsible for a close colocalization of the mutant AQP2 and Na-K-ATPase. When the same cells were pretreated with mouse anti-Na-K-ATPase antibody, anti-mouse IgG, but not anti-rabbit IgG, detected Na-K-ATPase (figures not shown), suggesting again absence of the cross-reaction.

Next, we examined the localization of the wild-type AQP2 and Na-K-ATPase in cells cotransfected with the wild-type and mutant AQP2s. After incubation with forskolin, the distribution of these proteins was similar to that observed in the mutant-transfected cells shown in Figure 3 (Fig. 4 A to C). The merged figure demonstrated colocalization of the wild-type AQP2 and Na-K-ATPase (Fig. 4C). When cells were preincubated with an antibody against the wild-type AQP2 (rabbit), the immunostaining of AQP2 was observed after incubation with anti-rabbit IgG (Fig. 4H), but not with anti-mouse IgG. (Fig. 4I), suggesting no cross-reactivity of these two antibodies. Similarly, the incubation with anti-mouse IgG, but not with anti-rabbit IgG, detected Na-K-ATPase in cells pretreated with mouse anti-Na-K-ATPase antibody (figures not shown). In general, AQPs are known to exist as tetramers at the plasma membrane. Therefore, we tested whether the wild-type and mutant AQP2s form oligomers by immunocytochemistry and immunoprecipitation. In cotransfected cells, double staining of the wild-type and mutant AQP2s showed a close localization (Fig. 4 D to F), suggesting the formation of mixed oligomers. The cross reaction of rat anti-wild-type AQP2 antibody and rabbit anti-mutant AQP2 antibody was excluded, because anti-rat IgG (Fig. 4J), but not anti-rabbit IgG (Fig. 4K), recognized the wild-type AQP2 in cells preincubated with anti-wild-type AQP2 antibody. Similarly, the mutant AQP2 was not identified by anti-rat IgG in cells preincubated with anti-mutant AQP2 antibody (figures not shown). When the membrane fractions of cotransfected cells were immunoprecipitated with an antibody against the wild-type AQP2, an antibody against the mutant AQP2 revealed a 34 kD band corresponding to the apparent molecular size of the mutant AQP2 (Fig. 5A). Furthermore, an anti-wild-type AQP2 antibody recognized a 29 kD band in the samples immunoprecipitated by an antimutant antibody (Fig. 5B), once more suggesting hetero-oligomerization. Taken together, our findings suggested that the mixed oligomers of the wild-type and mutant AQP2s were translocated to the basolateral surface, but not to the apical surface, due to the dominant-negative effect of the mutant.

Marr et al recently reported another AQP2 mutation in patients with autosomal-dominant NDI [8]. Their mutant (727delG) and our mutant (763 to 772del) share an identical C-terminal amino acids. They observed that the hetero-oligomer of the wild-type and 727delG AQP2s mainly localized to late endosomes/lysosomes in cotransfected cells [8]. Thus, we performed immunocytochemical studies in cells coexpressing the wild-type and 763-772del AQP2s. When cells were doubly stained with antibodies against ZO-1 and Lamp1, a marker of the late endosome/lysosome, fluorescence from Lamp1 was detected in the cytoplasm (Fig. 6 A to C). The cytoplasmic staining of Lamp1 was also seen in cells stained with antibodies against Na-K-ATPase and Lamp1 (Fig. 6 D to F). These findings suggested that the localization of Lamp1 seemed to differ from that of AQP2 hetero-oligomers that were essentially distributed at the basolateral membrane area (Fig. 4). Because both of our antibodies against the mutant AQP2 and Lamp1 were rabbit IgG, we were unable to detect the localization of these two proteins simultaneously in the present study.

DISCUSSION

The mutation of the mutant AQP2 used in this study is a deletion of 10 nucleotides starting at 763 (763 to 772del) in exon 4 of the *AQP2* gene [7]. The wild-type AQP2 is a 271 amino acid protein, whereas the 763 to 772del *AQP2* gene is predicted to encode 330 amino

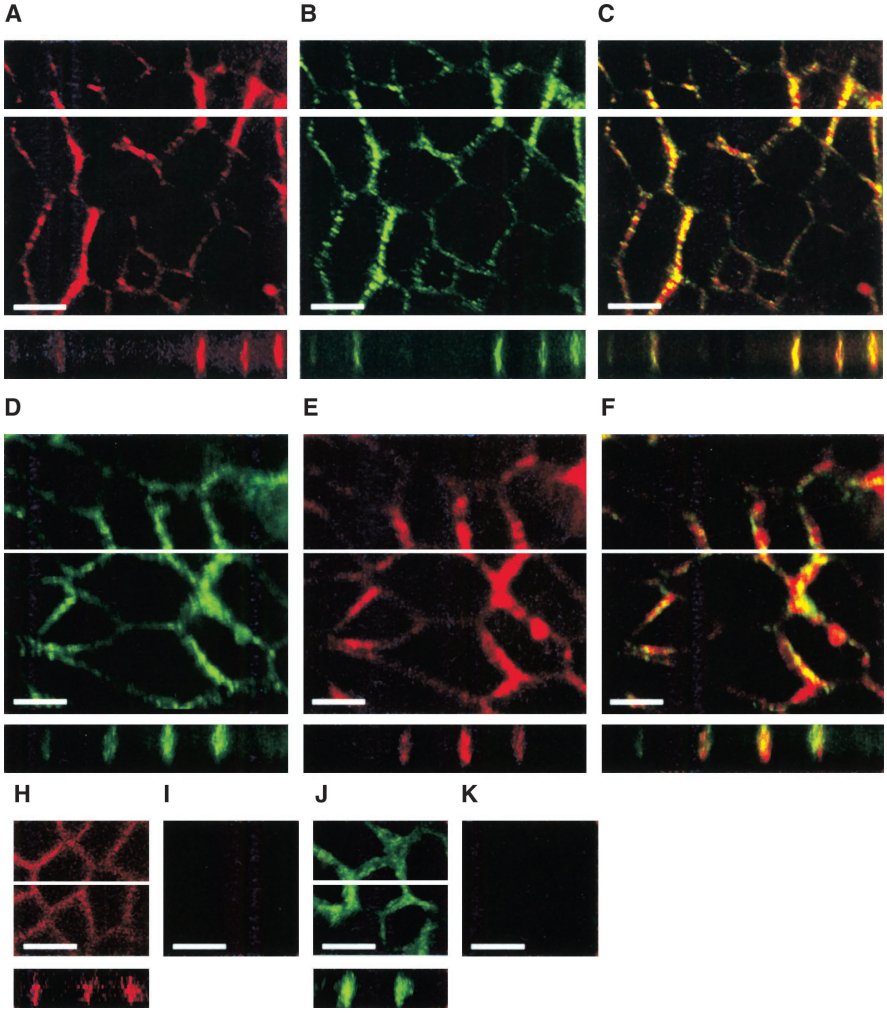

Fig. 4. Immunocytochemical localization of the wild-type and mutant aquaporin-2 (AQP2) in cotransfected Madin-Darby canine kidney (MDCK) cells. The wild-type and mutant AQP2s were stably cotransfected in MDCK cell. Colocalization of the wild-type AQP2 (*A*), Na-K-ATPase (*B*), and merged (*C*) was observed at ×400. Colocalization of the wild-type AQP2s (*D*), the mutant AQP2 (*E*), and merged (*F*) merged. Determination of the cross-reactivity of antibodies. Cells were incubated with rabbit anti-wild-type AQP2 antibody, and then incubated with antibodies against rabbit IgG (*H*) or mouse IgG *(I)*. In addition, cells were incubated with rat anti-wild-type AQP2 antibody, and then incubated with antibodies against rat IgG (*J*) or rabbit IgG *(K)*. XY and XZ sections are shown in the upper and lower panels, respectively. White bars indicate 10 μm.

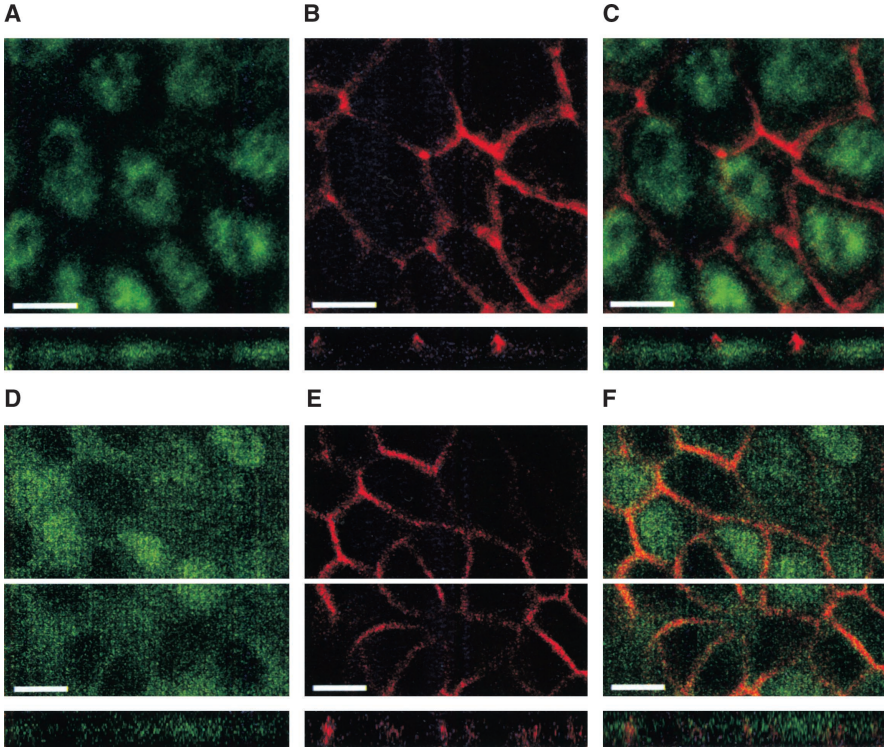

Fig. 6. Localization of Lamp1 in Madin-Darby canine kidney (MDCK) cells stably cotransfected with the wild-type and mutant aquaporin-2 (AQP2). Double staining of Lamp1 (*A*), ZO-1 (*B*), merged (*C*) or Lamp1 (*D*), Na-K-ATPase (*E*), or merged (*F*). XY and XZ sections are shown in the upper and lower panels, respectively. The samples were viewed at ×400 and white bars indicate 10 μm.

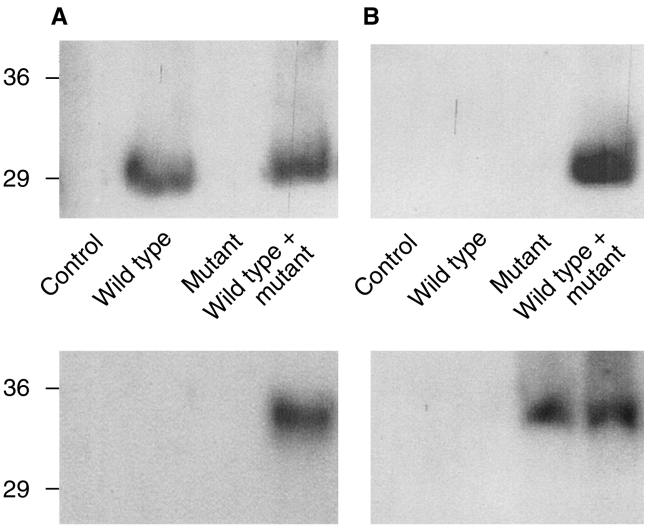

Fig. 5. Immunoprecipitation of the wild-type and mutant aquaporin-2 (AQP2) in cotransfected Madin-Darby canine kidney (MDCK) cells. (*A*) Samples were immunoprecipitated with a wild-type (WT) AQP2 antibody and immunoblotted with the same antibody (upper panel) or an antibody against mutant (M) AQP2 (lower panel). (*B*) Samples were immunoprecipitated with an antibody to the mutant AQP2 and immunoblotted with an antibody to the wild-type AQP2 (upper panel) or mutant AQP2 (lower panel).

acid proteins due to the frameshift mutation of the stop codon. Immunoblot analysis showed that the wild-type and mutant AQP2s were successfully transfected in MDCK cells (Fig. 1).

Transfected cells were grown to confluence on permeable support. The sorting of membrane channels/transporters in culture cells is generally thought to accelerate after the cells reach confluency, or more specifically, after cell polarity is rigidly established [10, 11]. Immunofluorescence microscopy suggested that the wild-type AQP2 was essentially localized at the apical membrane after forskolin treatment (Fig. 2). In contrast, the mutant AQP2 was apparently distributed at the lateral membrane (Fig. 3), with additional weak labeling of the basal membrane based on observations of the double staining with Na-K-ATPase. This difference of immunostaining in the lateral and basal membranes cannot be explained at present. However, a similar staining pattern was reported in the basolateral membrane proteins expressed in culture cells [12, 13]. In cotransfected cells, the wild-type and mutant AQP2s formed mixed oligomers that were predominantly distributed at the basolateral membrane (Figs. 4 and 5). These results suggested that the dominant-negative effect of the mutant is responsible for the mistargeting of the wild-type AQP2, leading to the pathogenesis of an autosomal-dominant–type NDI.

In cells before forskolin treatment, the wild-type AQP2 was mostly present at the apical membrane region (Fig. 2D), and apparently targeted to the apical membrane in response to forskolin (Fig. 2E). Immunoelectron microscopy of inner medullary collecting duct cells demonstrated the presence of AQP2 both in the apical plasma membrane and in small subapical vesicles, and the vasopressin-induced translocation of AQP2 to the apical membrane [14, 15]. Therefore, it might be possible that forskolin stimulated the apical trafficking of AQP2 distributed in the subapical region in our MDCK cell line. However, a detailed analysis of the protein localization was beyond the detection level of our immunocytochemistry. Immunoelectron microscopy will be necessary to prove our speculation. Contrary to cells grown on a membrane support, the wild-type AQP2 in MDCK cells grown on the coverglass was localized at perinuclear region as vesicle-like structure before forskolin treatment and homogenously localized to the apical membrane after the stimulation with forskolin [16] [unpublished observation by T. Asai). Such a characteristic distribution of AQP2 observed in cells on the coverglass might be due to the absence of rigid cell polarity. The mutant AQP2 was fundamentally present basolaterally before the incubation with forskolin (Fig. 3D). Furthermore, the red staining with antimutant AQP2 antibody was also detected just inside the lateral membrane in some cells as if a part of the mutant AQP2 were distributed there. Thus, comparison of Figure 3A and D suggested the possibility that forskolin accelerated basolateral trafficking of the mutant AQP2. However, further investigation will be required to confirm the effect of forskolin on the distribution of mutant AQP2 because our resolution of confocal microscopy is limited.

During the course of this study, Marr et al [8] reported another mutation that leads to autosomal dominant NDI in one allele of the *AQP2* gene. Interestingly, their mutant (727delG) and our mutant (763 to 772del) share an identical sequence of 66 amino acids at the C terminus. In the *Xenopus* oocyte expression system, they found that the wild-type and 727delG AQP2s formed hetero-oligomers and they were mostly retained within the cell [8]. They also reported that these hetero-oligomers were mainly localized at late endosomes/lysosomes when cotransfected in MDCK cells [8]. Our findings suggested that mixed oligomers of the wild-type and 763-772del AQP2s were basically distributed at the basolateral membrane region (Fig. 4), and apparently not predominantly localized in the late endosome/lysosome (Fig. 6), although the anti-Lamp1 antibody we used could not give a higher resolution. We cannot yet explain the reason for this discrepancy. Different sites of the mutations might explain the discrepancy. In a preliminary study, Kamsteeg et al reported another mutation (one-base insertion at C-terminus) in a patient with autosomal-dominant NDI [abstract; Kamsteeg et al, *J Am Soc Nephrol* 12:304A, 2001]. This mutation led to a replacement of the 12 C-terminal amino acids of the wild-type

AQP2 with a new C-terminal tail of 26 amino acids (QLAAEPATGYQGLRAASGLYGPDGRF). In expression studies in MDCK cells, Kamsteeg's group found basolateral localization of the mutant AQP2 and suggested that some of the amino acids at the new C-terminal were responsible for the mistargeting.

The E258K in the *AQP2* gene is the first mutation reported for autosomal-dominant NDI [5]. In contrast to the 763 to 772del mutation, the E258K mutation resulted in a retention of the mixed tetramers in the Golgi compartment in the *Xenopus* oocyte expression system [5, 6]. In most forms of autosomal-recessive NDI due to *AQP2* gene mutations, mutant proteins were misfolded and retained in endoplasmic reticulum as a monomer and not further transported to Golgi apparatus [17, 18]. A similar endoplasmic reticulum retention of misfolded proteins had been demonstrated in a number of X-linked recessive NDI cases due to *AVPR2* gene mutations [2, 3]. In addition to NDI, protein trafficking defects are also known to be responsible for a large member of congenital diseases. For example, the deltaF508 mutation found in the *CFTR* gene of cystic fibrosis patients causes protein degradation in the endoplasmic reticulum [19]. Moyer et al [20] presented evidence that the last three amino acids at the C-terminus (T-R-L) of the cystic fibrosis transmembrane conductance regulator (CFTR) comprise a PDZ-interacting domain that binds to ezrin-radixin-moesin-binding phosphoprotein 50 (EBP50), a protein that contains the PDZ domain [20]. This interaction seemed to be requisite for the apical membrane polarization of CFTR, as the S1455X CFTR mutant lacking the 26 C-terminal amino acids was mistargeted to the basolateral membrane and thereby led to the pathogenesis of cystic fibrosis [20]. In Charcot-Marie-Tooth disease, mutations of peripheral myelin protein 22 or connexin 32 lead to accumulation of the mutant protein in the endoplasmic reticulum/Golgi compartment [21, 22]. Several types of defects are known in familial hypercholesterolaemia; namely, failure to exit the endoplasmic reticulum in class 2, failure to cluster in coated pits in class 4, and failure to recycle after endocytosis in class 5 [23]. Thus, we can speculate that heterogeneous mechanisms are involved in the defects of intracellular protein trafficking.

Our results suggested that mixed oligomers of the wild-type and mutant AQP2s are mistargeted to the basolateral membrane, as well as the mutant AQP2 itself (Figs. 3 and 4). A similar molecular pathogenesis of hereditary diseases was shown only in cystic fibrosis due to the S1455X CFTR mutant, as described above. We propose two possible explanations for the mistrafficking in our case. The mutation causes either a loss of the apical targeting determinant, or an addition of a basolateral targeting determinant that dominates the intrinsic apical targeting determinant. Several determinants have been found for apical targeting. In the case of protein anchored to the cell membrane via glycerol-phosphatidylinositol (GPI), the glycolipid moiety is thought to act as an apical sorting signal [24]. However, AQP2 is not known as a GPI-anchored protein. A cluster of membrane proteins is known to move from the trans-Golgi network (TGN) to the apical surface with rafts composed of a detergent-insoluble glycolipid (DIG)-enriched complex [25]. A certain transmembrane domain is thought to interact with rafts [25]. In addition, protein traffic is generally mediated by the soluble N-ethylmaleimide-sensitive factor attachment protein (SNARE) machinery [26, 27]. Numerous SNARE-related proteins are shown to be involved in protein sorting. In the case of AQP2, vesicle-associated membrane protein 2 (VAMP2) [28], and syntaxin-4 [29] were reported to colocalize with AQP2 in the collecting duct cells. For basolateral targeting determinants in TGN, tyrosine-related and dileucine-related motifs were identified as signals to regulate localization of clathrin-coated vesicles [24]. Indeed, the sorting of AQP4 to the basolateral surface has been shown to depend on these two motifs [30]. The elongated C-terminal of our mutant AQP2 contains one dileucine motif but no tyrosine residues. Thus, the underlying mechanism of mistargeting observed in the mutant AQP2 remains unknown, and the several possibilities proposed above remain untested. Further investigations will seek to clarify the cause for this mistargeting in our NDI case.

ACKNOWLEDGMENTS

We thank Dr. E. Kominami for providing us an antibody against Lamp1. This work was supported by a Grant-in-Aid for Scientific Research and Grant-in-Aid for Scientific Research on Priority Areas from Japan Society for the Promotion of Science (JSPS).

Reprint requests to Michio Kuwahara, M.D., Department of Homeostasis Medicine and Nephrology, Graduate School, Tokyo Medical and Dental University, Tokyo 113-8519, Japan.
E-mail: mkuwahara.kid@tmd.ac.jp

REFERENCES

1. Fushimi K, Uchida S, Hara Y, *et al*: Cloning and expression of apical membrane water channel of rat kidney collecting tubule. *Nature* 361:549–552, 1993
2. Morello J-P, Bichet DG: Nephrogenic diabetes insipidus. *Annu Rev Physiol* 63:607–630, 2001
3. Nielsen S, Frokiaer J, Marples D, *et al*: Aquaporins in the kidney. *Physiol Rev* 82:205–244, 2002
4. Deen PMT, Verdijk MAJ, Knoers NVAM, *et al*: Requirement of human renal water channel aquaporin-2 for vasopressin-dependent concentration of urine. *Science* 264:92–95, 1994
5. Mulders SM, Bichet DG, Rijss JPL, *et al*: An aquaporin-2 water channel mutant which causes autosomal dominant nephrogenic diabetes insipidus is retained in the Golgi complex. *J Clin Invest* 102:57–66, 1998
6. Kamsteeg E-J, Wormhoudt TAM, Rijss JPL, *et al*: An impaired routing of wild-type aquaporin-2 after tetramerization with an aquaporin-2 mutant explains dominant nephrogenic diabetes insipidus. *EMBO J* 18:2394–2400, 1999
7. Kuwahara M, Iwai K, Ooeda T, *et al*: Three families with autosomal dominant nephrogenic diabetes insipidus caused by aquaporin-2 mutations in the C-terminus. *Am J Hum Genet* 69:738–748, 2001

8. Marr N, Bichet DG, Lonergan M, *et al*: Heteroligomerization of an aquaporin-2 mutant with wild-type aquaporin-2 and their misrouting to late endosomes/lysozomes explains dominant nephrogenic diabetes insipidus. *Hum Mol Genet* 11:779–789, 2002
9. Lefebvre B, Formstecher P, Lefebvre P: Improvement of the gene splicing overlap (SOE) method. *Biotechniques* 19:186–188, 1995
10. Handler JS: Use of cultured epithelia to study transport and its regulation. *J Exp Biol* 106:55–69, 1983
11. Horster MF, Stopp M: Transport and metabolic functions in cultured renal tubule cells. *Kidney Int* 29:46–53, 1986
12. Keller P, Toomre D, Diaz E, *et al*: Multicolor imaging of post-Golgi sorting and trafficking in live cells. *Nat Cell Biol* 3:140–149, 2001
13. Dillon C, Creer A, Kerr K, *et al*: Basolateral targeting of ERBB2 is dependent on a novel bipartite juxtamembrane sorting signal but independent of the C-terminal ERBIN-binding domain. *Mol Cell Biol* 22:6553–6563, 2002
14. Nielsen S, DiGiovanni SR, Christensen EI, *et al*: Cellular and subcellular immunolocalization of vasopressin-regulated water channel in rat kidney. *Proc Natl Acad Sci USA* 90:11663–11667, 1993
15. Nielsen S, Chou C-L, Marples D, *et al*: Vasopressin increases water permeability of kidney collecting duct by inducing translocation of aquaporin-CD water channels to plasma membrane. *Proc Natl Acad Sci USA* 92:1013–1017, 1995
16. Deen PMT, Rijss JPL, Mulders SM, *et al*: Aquaporin-2 transfection of Madin-Darby canine kidney cells reconstitutes vasopressin-regulated transcellular osmotic water transport. *J Am Soc Nephrol* 8:1493–1501, 1997
17. Mulders SM, Knoers NV, Van Lieburg AF, *et al*: New mutations in the AQP2 gene in nephrogenic diabetes insipidus resulting in functional but misrouted water channels. *J Am Soc Nephrol* 8:242–248, 1997
18. Marr N, Bichet DG, Hoefs S, *et al*: Cell-biologic and functional analysis of five new aquaporin-2 missense mutations that cause recessive nephrogenic diabetes insipidus. *J Am Soc Nephrol* 13: 2267–2277, 2002
19. Cheng SH, Gregory RJ, Marshall J, *et al*: Defective intracellular transport and processing of CFTR is the molecular basis of most cystic fibrosis. *Cell* 63:827–834, 1990
20. Moyer BD, Denton J, Karlson KH, *et al*: A PDZ-interacting domain in CFTR is an apical membrane polarization signal. *J Clin Invest* 104:1353–1361, 1999
21. Sanders CR, Ismail-Beigi F, McEnery MW: Mutations of peripheral myelin protein 22 result in defective trafficking through mechanisms which may be common to diseases involving tetraspan membrane proteins. *Biochemistry* 40:9453–9459, 2001
22. Abrams CK, Oh S, Ri Y, *et al*: Mutations in connexin 32: The molecular and biophysical bases for the X-linked form of Charcot-Marie-Tooth disease. *Brain Res Brain Res Rev* 32:203–214, 2000
23. Hobbs HH, Russell DW, Brown MS, *et al*: The LDL receptor locus in familial hypercholesterolemia: Mutational analysis of a membrane protein. *Annu Rev Genet* 24:133–170, 1990
24. Matter K, Mellman I: Mechanisms of cell polarity: sorting and transport in epithelial cells. *Curr Opin Cell Biol* 6:545–554, 1994
25. Harder T, Simons K: Caveolae, DIGs, and the dynamics of sphingolipid-cholesterol microdomains. *Curr Opin Cell Biol* 9:534–542, 1997
26. Rothman JE, Warren G: Implications of the SNARE hypothesis for intracellular membrane topology and dynamics. *Curr Biol* 4:220–233, 1994
27. Hay JC, Scheller RH: SNAREs and NSF in targeted membrane fusion. *Curr Opin Cell Biol* 9:505–512, 1997
28. Nielsen S, Marples D, Mohtashami M, *et al*: Expression of VAMP2-like protein in kidney collecting duct intracellular vesicles: Co-localization with aquaporin-2 water channels. *J Clin Invest* 96:1834–1844, 1995
29. Mandon B, Chou C-L, Nielsen S, *et al*: Syntaxin-4 is localized to the apical plasma membrane of rat renal collecting duct cells: possible role in aquaporin-2 trafficking. *J Clin Invest* 98:906–913, 1996
30. Madrid R, Le Maout S, Barrault M-B, *et al*: Polarized trafficking and surface expression of the AQP4 water channel are coordinated by serial and regulated interactions with different clathrin-adaptor complexes. *EMBO J* 20:7008–7021, 2001